



Research article

Konjac glucomannan defends against high-fat diet-induced atherosclerosis in rabbits by promoting the PI3K/Akt pathway

Junting Weng^a, Min Chen^a, Bingbing Shi^a, Danjuan Liu^a, Shuoyun Weng^b, Rongjie Guo^{a,*}

^a Department of Critical Care Medicine, The Affiliated Hospital of Putian University, Putian 351100, China

^b School of Wenzhou Medical University, Wenzhou 325035, China



ARTICLE INFO

Keywords:

Konjac glucomannan
Atherosclerosis
Endothelial function
VCAM-1
Oxidative stress
PI3K/Akt pathway

ABSTRACT

Atherosclerosis (AS) is the main cause of cardiovascular disease and cerebral infarction, which seriously endanger human health. This study aimed to investigate konjac glucomannan (KGM) defends against high-fat diet-induced AS in rabbits by promoting the PI3K/Akt pathway. KGM administration reduced the degree of AS indicated by reducing the plaques and foam cells, the tunica intima thickness, and the tunica intima/tunica media thickness ratio in the aorta, and enlarging the lumen of the aorta. In addition, KGM administration regulated blood lipids, ameliorated inflammation indicated by reducing the levels of tumor necrosis factor-alpha (TNF- α), interleukin (IL)-6, CRP, and VCAM-1, and attenuated endothelial injury, simultaneously mitigated oxidative stress indicated by decreasing MPO activity and the concentrations of MDA and increasing the GSH-Px and SOD concentrations. Moreover, KGM promotes the phosphorylation of PI3K and AKT. However, these effects of KGM on rabbits with high-fat diet-induced AS were blocked by LY294002. In conclusion, KGM defends against high-fat diet-induced AS in rabbits by promoting the PI3K/Akt pathway.

1. Introduction

Atherosclerosis (AS) is the main cause of cardiovascular disease and cerebral infarction, which seriously endanger human health [1]. Atherosclerosis attracts attention because of its high morbidity, disability, and mortality. Atherosclerotic cardiovascular disease (CVD) has spread worldwide. In 2015, 17 million people died from cardiovascular disease, representing 31% of all global deaths [2]. AS has always been a target in cardiovascular and cerebrovascular disease prevention and treatment. Therefore, how to intervene in the occurrence and development of atherosclerosis to reduce the incidence of cardiovascular and cerebrovascular diseases is a current research hotspot. Statins are commonly used as lipid-regulating and antiatherosclerosis drugs at present [3], but their extensive clinical application is limited due to their side effects, such as liver dysfunction and rhabdomyolysis. Therefore, finding an antiatherosclerosis drug with high safety and few side effects will help reduce the incidence of cardiovascular and cerebrovascular diseases.

Konjac glucomannan (KGM), which is a soluble dietary fiber, is used as a component of supplements for weight loss [4]. KGM is a reserve polysaccharide contained in the konjac tuber, is a polymer compound formed by the binding of glucose and mannose through β -1, 4 glycosidic bonds, is an excellent kind of dietary fiber, and has good water retention, gelling, and thickening properties [5]. Studies

* Corresponding author. No. 999 Dongzhen East Road, Licheng District, Putian, Fujian, China.

E-mail addresses: juntingweng@126.com (J. Weng), minchen1980@126.com (M. Chen), bingbinshi@126.com (B. Shi), danjuanliu@126.com (D. Liu), shuoyunweng8618@163.com (S. Weng), rongjieguo1109@126.com (R. Guo).

<https://doi.org/10.1016/j.heliyon.2023.e13682>

Received 10 October 2022; Received in revised form 4 February 2023; Accepted 7 February 2023

Available online 13 February 2023

2405-8440/© 2023 The Authors. Published by Elsevier Ltd. This is an open access article under the CC BY-NC-ND license (<http://creativecommons.org/licenses/by-nc-nd/4.0/>).

Nomenclature

ANOVA	one-way analysis of variance
AS	atherosclerosis
Akt	protein kinase B
KGM	konjac glucomannan
DF	dietary fiber
CTR	control group
CRP	C- reactive protein
ET	Endothelin
HDL-C	High-density lipoprotein cholesterol
LDL-C	Low-density lipoprotein cholesterol
NO	Nitric oxide
TC	Total cholesterol
TG	Triglycerides
VCAM-1	Vascular cell adhesion molecule-1
PI3K	phosphatidylinositol 3-kinase
MPO	myeloperoxidase
MDA	malondialdehyde
SOD	superoxide dismutase
GSH-Px	glutathione peroxidase

have reported that it can reduce body weight, prevent and cure hypertension, increase insulin sensitivity, and exert anti-inflammatory, antioxidation, and other effects [6]. KGM can make the contents of the stomach and small intestine sticky, delay gastric emptying, and thicken the unagitated layer in the small intestine (fluid gel film), thus slowing down the absorption of cholesterol in the intestine. Moreover, KGM can bind to bile acid, inhibit cholesterol reabsorption in the intestine, reduce the enterohepatic circulation of cholesterol, and thus increase the cholesterol metabolism speed, providing a cholesterol-lowering effect [7]. Therefore, the role and mechanism of KGM in atherosclerosis are worth studying.

In recent years, an increasing number of studies have confirmed that the PI3K/AKT pathway is significantly associated with the pathogenesis of AS. Yan et al. [8] confirmed that the PI3K/AKT signaling pathway can regulate the important cellular biological bases of the pathogenesis of AS, such as the vascular endothelium, vascular smooth muscle cells, platelets, and macrophages. The PI3K/Akt signaling pathway is a key signaling pathway that regulates cell proliferation, differentiation, apoptosis, and senescence. PI3K is a heterodimer that acts as a mediator between extracellular signaling and cellular responses [9].

In the present study, we hypothesized that KGM alleviates high-fat diet-induced atherosclerosis in rabbits by promoting the PI3K/Akt pathway.

2. Materials and methods

2.1. Experimental animals

A total of 32 healthy male rabbits aged approximately 4 months, with a bodyweight of 2.00 ± 0.15 kg, were provided by the Experimental Animal Center of Fujian Medical University. They were kept in cages and given free access to drinking water. The feeding environment of all rabbits was the same. The feeding limit for each rabbit was 110–130 g/d. Animal protocols were completed according to the Guide for the Care and Use of Laboratory Animals published by the US National Institutes of Health and were approved by the Ethics Committee of the Affiliated Hospital of Putian University.

2.2. Materials

KGM was purchased from Hubei Xiangfan Huipu Biochemical Science and Technology Engineering Co., Ltd. A cholesterol kit was purchased from Beckman Reagents, Inc. An endothelin kit was purchased from Tianjin Chiye Biological Products Co., Ltd. The nitric oxide kit was purchased from the Nanjing Jiancheng Institute of Biological Engineering. The rabbit anti-VCAM-1 polyclonal antibody was purchased from Wuhan Bode Biological Engineering Co., Ltd. An S-P immunohistochemical kit was purchased from Wuhan Bode Biological Engineering Co., Ltd. A DAB color kit was purchased from Wuhan Bode Biological Engineering Co., Ltd. LY294002 was purchased from Med Chem Express, Company.

2.3. Experimental methods

2.3.1. Experimental grouping and treatment methods

Thirty-two rabbits were randomly divided into 4 groups with 8 rabbits in each group. The control group (CTR) was supplied with a

normal diet for 12 weeks. The high-fat model group (HFD) was supplied with a high-fat diet (formula: 91% ordinary diet +1% cholesterol +8% lard) for 12 weeks. Konjac glucomannan group (KGM) was fed a high-fat diet with 7.5% konjac glucomannan 300 mg/kg/d for 12 weeks. The KGM + LY group (KGM + LY) was fed a high-fat diet supplemented with 7.5% KGM 300 mg/kg/d for 12 weeks and received LY294002 (3 mg/kg 2 times a week for 2 weeks) via peritoneal injection beginning at the 10th week. After 12 weeks, the rabbits in each group were euthanized to obtain blood and specimens.

2.4. Observation indices and detection methods

2.4.1. Blood lipid test

At the end of the 12th week, 3 ml of fasting blood samples (fasting for 12 h) were taken from the central ear artery of the rabbits and centrifuged (3000 rpm, 10 min). Serum was extracted, and Total cholesterol (TC), Triglycerides (TG), Low-density lipoprotein cholesterol (LDL-C), and High-density lipoprotein cholesterol (HDL-C) were determined by the oxidase method using a Mindray automatic biochemical analyzer.

2.4.2. Detection of serum concentrations of inflammatory factor

The blood sampling time was the same as the above. The CRP, TNF- α , and IL-6 concentrations were determined by ELISA.

2.4.3. Detection of serum concentrations of endothelial function

The ET concentrations were determined by ELISA. The NO concentration was determined by the nitrate reductase method.

2.4.4. Pathomorphological observation

After the experiment, all rabbits were anesthetized with pentobarbital sodium (1%) and killed.

- (1) The aorta from the beginning of the aortic arch to the anterior iliac bifurcation of the abdominal aorta was immediately removed, the extracapsular connective tissue and fat were removed from the aorta, and residual blood was rinsed away with normal saline.
- (2) In each group, the aorta beginning 2 cm below the aortic arch was cut longitudinally along the long axis, residual blood was flushed away with normal saline, and the vascular strips were placed in 10% formaldehyde solution for fixation for 45–60 min.
- (3) The vascular strips were removed from the formaldehyde solution, rinsed with normal saline, and stained with Sudan III for 10 min.
- (4) The vascular strips were removed from the staining solution, rinsed with normal saline, and paved. The AS plaques exhibited an orange color.
- (5) A 1 cm aorta sample was cut from the aortic arch and fixed in a neutral formaldehyde solution for 24 h. The cross-section was collected, dehydrated, embedded in paraffin, and cut into 5 μ m sections, which were stained with hematoxylin-eosin (H&E).
- (6) A Olympus light microscope with 100-times magnification was used to observe the morphology of the pathological sections, and a CIAS-100 cell image analyzer was used.
- (7) The thicknesses of the tunica intima and tunica media of the aorta were measured at 5 different locations randomly selected from the sections of each specimen, the average value was taken as the detection value of each specimen, and the tunica intima/tunica media thickness ratio was calculated.

2.4.5. Positive expression of VCAM-1 in the aortic wall analysis by immunohistochemistry

The SP method was used with DAB staining. The main operational steps were as follows:

- (1) After dewaxing and hydration, each aortic specimen was rinsed with PBS solution (pH 7.4) 3 times for 5 min each.
- (2) Citric acid was used for high-pressure repair for 2 min, followed by natural cooling and rinsing with PBS 3 times for 5 min each.
- (3) Each section was successively added to 50 μ L peroxidase blocking solution (reagent A) and normal nonimmune animal serum (reagent B) and incubated at room temperature for 10 min in each.
- (4) The serum was removed, and 50 μ L mouse anti-rabbit VCAM-1 polyclonal antibody (primary antibody, 1:100) was added and incubated with the sample at room temperature for 60 min or 4 °C overnight.
- (5) The sections were rinsed with PBS solution 3 times for 5 min each, and 50 μ L biotin-labeled sheep anti-rabbit antibody IgG (secondary antibody) was added. After incubation for 10 min, 50 μ L Streptomyces biotin-peroxidase solution was added.
- (6) Finally, 100 μ L freshly prepared DAB solution was added for DAB staining. The slides were dehydrated and dried in an alcohol gradient, xylene was used to make the sections transparent, and neutral gum was used to seal the slides.
- (7) The brown-yellow granular products were observed as positive markers under a microscope, and the percentage of positive-staining markers was calculated by automatic analysis with cell image analysis software.

2.4.6. Measurement of artery MPO and serum MDA, superoxide dismutase (SOD), and glutathione peroxidase (GSH-px)

The levels of MPO, MDA, SOD, and GSH-px were analyzed using ELISA kits following the manufacturer's instructions.

2.4.7. Western blot analysis

A protease inhibitor cocktail supplemented with radio-immunoprecipitation assay (RIPA) buffer was used to extract protein from

aortic tissues. A BCA analysis kit was used to determine the protein levels of the whole lysate after brief sonication and rotation (15,000 rpm, 15 min, 4 °C). The protein lysates were then mixed with 2-mercaptoethanol and heated at 95 °C for 5 min to denature the proteins. Following this, the denatured samples were separated over a 2-h period using 10% polyacrylamide gel electrophoresis (PAGE). The resolved proteins were then put on a polyvinylidene difluoride (PVDF) membrane (0.2 μm) and run at 100 V for 2 h in a refrigerated environment. The blots were blocked with nonfat milk (5%) in tris-buffered saline with 0.1% Tween 20 detergent (TBST) for 1 h at 25 °C, and the primary antibodies then interacted with the membrane for an overnight period at 4 °C. The membranes were then thoroughly cleaned before being incubated with HRP-conjugated secondary antibodies at 25 °C for 1 h. Thermo Fisher's iBright Western blot imaging system was then utilized to produce a digital image of the blots, which was then analyzed and quantified using Image J software. $P\text{-Akt}/\text{Akt ratios} = \text{gray-scale value of P-Akt}/\text{gray-scale value of Akt} \times 100\%$.

2.5. Statistical analysis

All data are expressed as the mean \pm standard deviation. The statistical software GraphPad Prism Software Version 8.0 was used for data analysis and processing. One-way analysis of variance (ANOVA) was used for comparisons between multiple groups, and the Q test was used for comparisons between two groups. $P < 0.05$ was considered statistically significant. The pathomorphological data were analyzed by contrast description.

3. Results

3.1. Impacts of KGM and LY294002 on blood lipids in rabbits with high-fat diet-induced atherosclerosis

To observe the effect of KGM and LY294002 on blood lipids, our study measured the serum concentrations of TC, TG, LDL-C, and

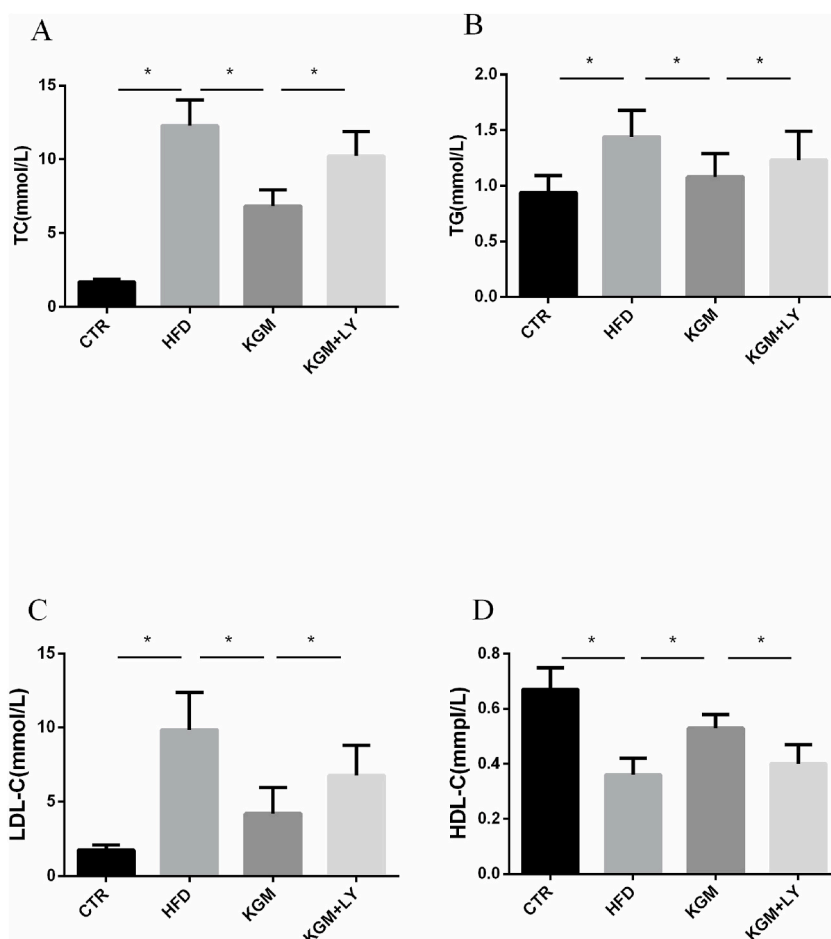


Fig. 1. Impacts of KGM and LY294002 on blood lipids in rabbits with high-fat diet-induced atherosclerosis. TC(A), TG(B), LDL-C(C), and HDL-C(D) were determined by the oxidase method using a Mindray automatic biochemical analyzer. The results are expressed as the mean \pm standard deviation (n = 8). *P < 0.05 vs. the indicated groups. KGM = konjac glucomannan.

HDL-C. Compared with the CTR group, TC, TG, and LDL-C in the HFD group were significantly increased ($P < 0.05$), while HDL-C in the HFD group was significantly decreased ($P < 0.05$). However, KGM administration dramatically increased the levels of HDL-C, while reduced the levels of TC, TG, and LDL-C ($P < 0.05$). Noteworthy, LY blocked the effects of KGM on blood lipids in rabbits with high-fat

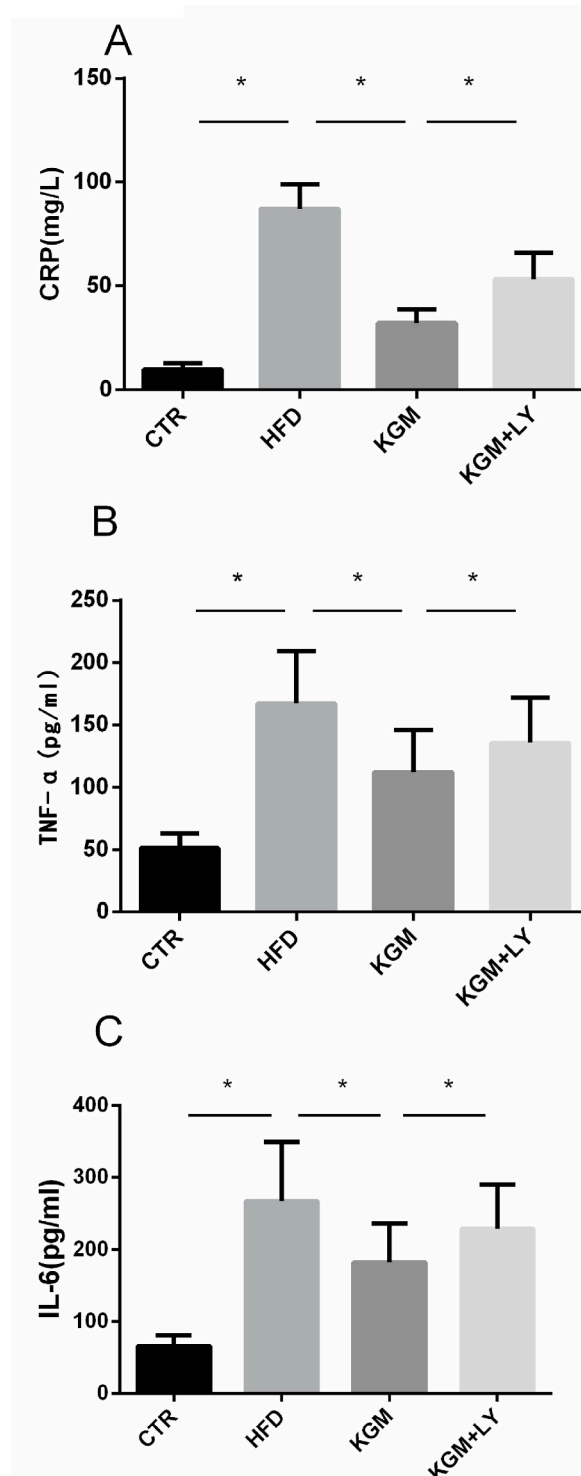


Fig. 2. Impacts of KGM and LY294002 on the inflammatory response in rabbits with high-fat diet-induced atherosclerosis rabbits. The concentrations of CRP(A), TNF- α (B), and IL-6(C) were determined by ELISA. The results are expressed as the mean \pm standard deviation ($n = 8$). * $P < 0.05$ vs. the indicated groups. KGM = konjac glucomannan.

diet-induced atherosclerosis ($P < 0.05$). The results are shown in Fig. 1A–D.

3.2. Impacts of KGM and LY294002 on the inflammatory response in rabbits with high-fat diet-induced atherosclerosis

To observe the effect of KGM and LY294002 on the inflammatory response, our study measured the Serum concentrations of CRP, TNF- α , and IL-6. Compared with the CTR group, CRP, TNF- α , and IL-6 in the HFD group were significantly increased ($P < 0.05$). Noteworthy, KGM administration significantly decreased the levels of CRP, TNF- α , and IL-6 compared with the HFD group ($P < 0.05$). Nevertheless, compared with the KGM group, CRP, TNF- α , and IL-6 in the KGM + LY group were significantly increased ($P < 0.05$). The results are shown in Fig. 2A–C.

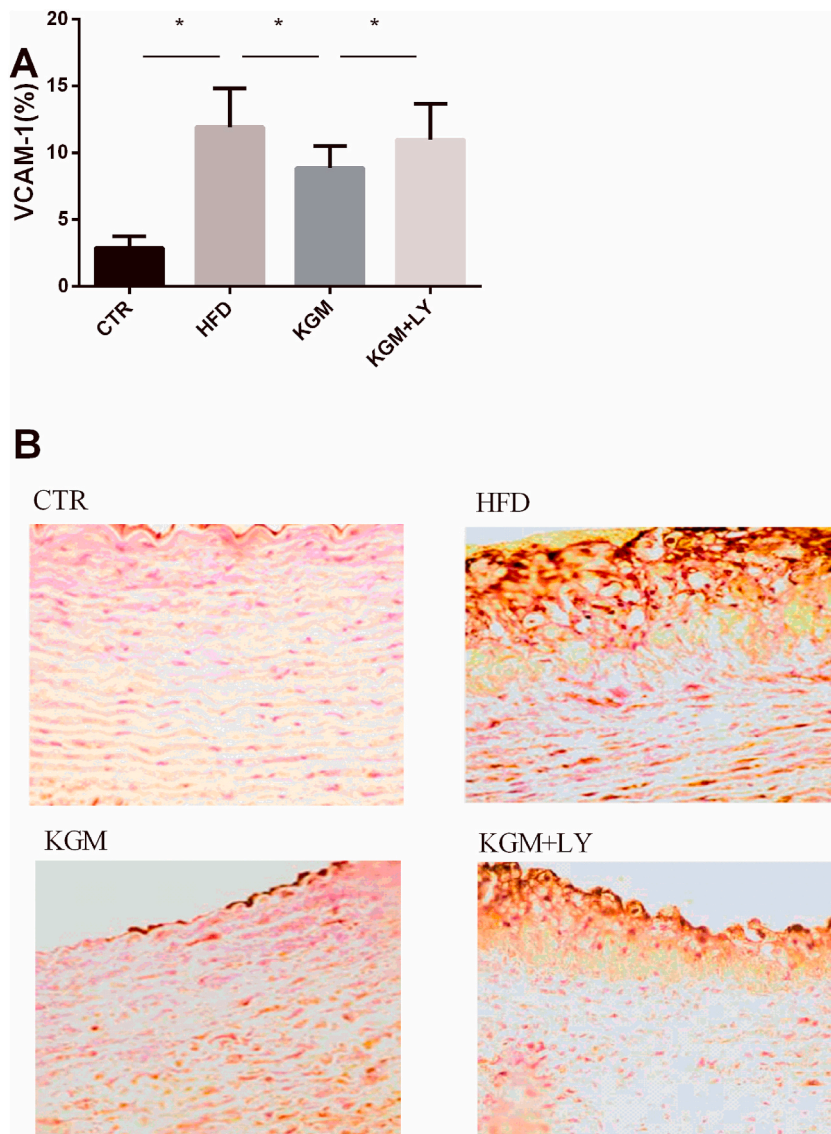


Fig. 3. Impacts of KGM and LY294002 on the positive expression of VCAM-1 in rabbits with high-fat diet-induced atherosclerosis. (A) Positive expression of VCAM-1 in the aortic wall was analyzed by immunohistochemistry. The brown-yellow granular products were observed as positive markers under the microscope, and the percentage of positive staining markers was calculated by automatic analysis with cell image analysis software. (SP method, DAB staining). (B) Characteristic blots of positive VCAM-1 of expression. The results are expressed as the mean \pm standard deviation ($n = 8$). * $P < 0.05$ vs. the indicated groups. KGM = konjac glucomannan. (For interpretation of the references to color in this figure legend, the reader is referred to the Web version of this article.)

3.3. Impacts of KGM and LY294002 on the positive expression of VCAM-1 in rabbits with high-fat diet-induced atherosclerosis

To examine whether KGM reduced AS, our study determined the positive expression of VCAM-1. Relative to the CTR group, the positive expression of VCAM-1 in the HFD group was significantly increased ($P < 0.05$). Relative to the HFD group, the positive expression of VCAM-1 in the KGM group was significantly decreased ($P < 0.05$). To further observe the underlying effects of the PI3K/Akt signal on the defensive roles of KGM, we explored whether LY294002 administration influenced the positive expression of VCAM-1 in high-fat diet-induced atherosclerosis rabbits. The positive expression of VCAM-1 in the KGM + LY group was significantly increased compared with that in the KGM group ($P < 0.05$). The results are shown in Fig. 3A and B.

3.4. Impacts of KGM and LY294002 on endothelial function in rabbits with high-fat diet-induced atherosclerosis

To examine whether KGM improved endothelial function, we determined the serum concentrations of NO and ET. Compared with the CTR group, NO in the HFD group was significantly decreased, while ET in the HFD group was significantly higher ($P < 0.05$). Noteworthy, KGM administration increased NO levels and decreased ET levels significantly. Whereas, LY administration inhibited the effect of KGM on endothelial function (As illustrated in Fig. 4A and B).

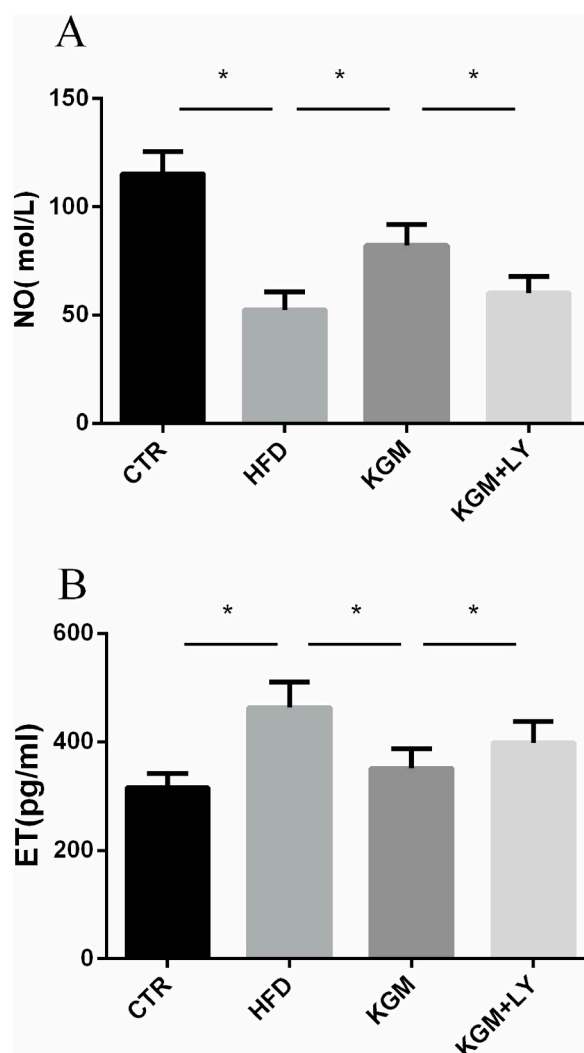


Fig. 4. Impacts of KGM and LY294002 on endothelial function in rabbits with high-fat diet-induced atherosclerosis. (A) NO concentrations were determined by the nitrate reductase method. (B) ET concentrations were determined by ELISA. The results are expressed as the mean \pm standard deviation ($n = 8$). * $P < 0.05$ vs. the indicated groups. KGM = konjac glucomannan.

3.5. Impacts of KGM and LY294002 on pathological changes in the aorta in rabbits with high-fat diet-induced atherosclerosis

To observe the role of KGM and LY294002 on AS, we determined the pathological changes in the aorta.

Gross observations indicated that the intimal surface of the aorta in the CTR group was smooth, thin, pink, and white, without the formation of lipid plaques, and no orange Sudan III staining was observed (the AS area was 0). The intima of the aorta in the HFD group was rough and thickened. After staining, the orange plaques protruded into the official cavity, and some protrusions were fused into the slices. In the KGM group, only a small number of lipid plaques and streaks were formed in the intima of the aorta, and most of the intima were smooth. Conversely, Lipid plaques and streaks formed in the intima of the aorta in the KGM + LY group were significantly increased compared with those in the KGM group ($P < 0.05$). The results are shown in Fig. 5A.

Optical microscope observations indicated that the aortic vessels in the CTR group were stratified, the intima was complete, the endothelium was continuous, the smooth muscle cells were in good condition, and there was no foam cell deposition in the inner

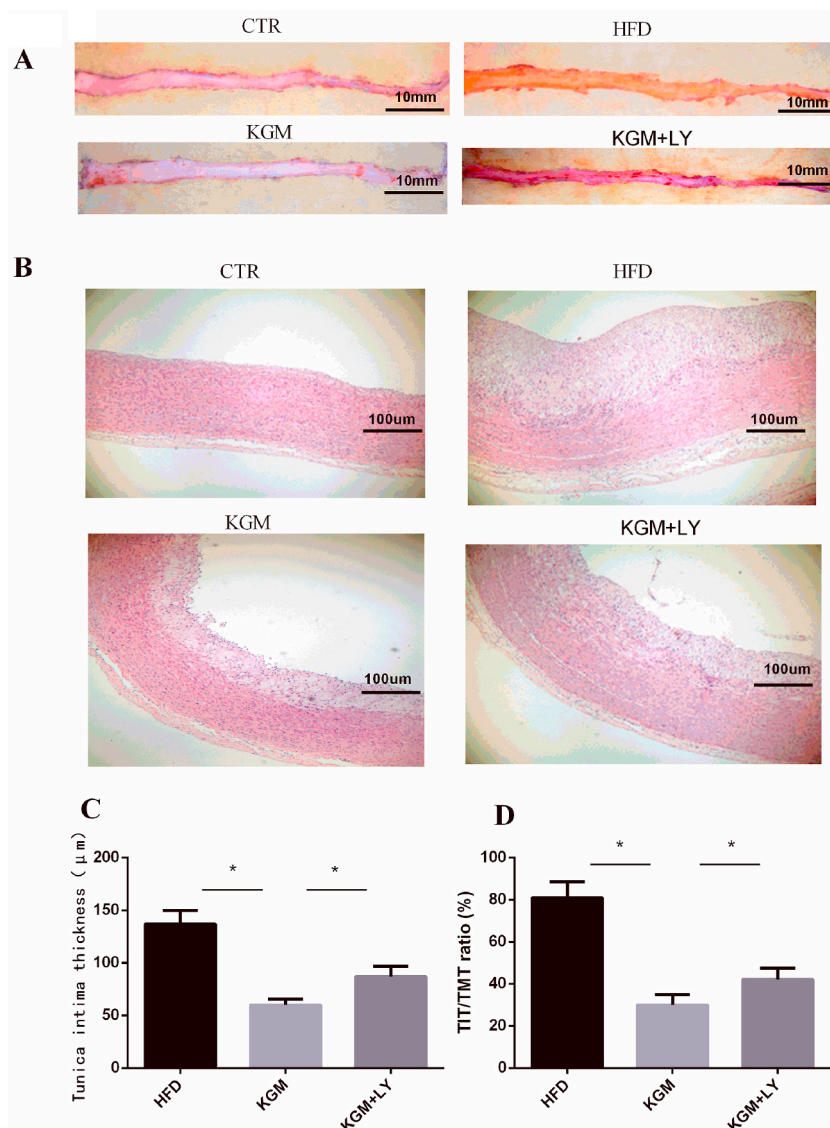


Fig. 5. Impacts of KGM and LY294002 on pathological changes in the aorta in rabbits with high-fat diet-induced atherosclerosis. (A) Macroscopic pathology of the aorta (Sudan III staining), with AS patches are shown in orange-red. (B) Characteristic pathological images after H&E staining. The structure of the aorta in the CTR group was clear, and the intima was smooth. The intima of the aorta in the HFD group was thickened and contained a large number of foam cells. In the KGM group, the intima of the aorta was thickened and reduced, and a few foam cells were present. (C) Thicknesses of the tunica intima of the aorta were measured by a CIAS-100 cell image analyzer. (D) Tunica intima thickness/tunica media thickness ratio (TIT/TMT ratio) was calculated. The results are expressed as the mean \pm standard deviation ($n = 8$). * $P < 0.05$ vs. the indicated groups. KGM = konjac glucomannan. (For interpretation of the references to color in this figure legend, the reader is referred to the Web version of this article.)

subcutaneous area. In the HFD group, the thickening of the intima was the most significant, with a large number of foam cells, a discontinuous endothelium, a disordered arrangement of smooth muscle cells, and a narrowing of the lumen ($P < 0.05$). Interestingly, Compared with the HFD group, KGM administration attenuated the thickness of aortic intima, foam cells, and lipids in the plaques, and the thickness of the tunica intima and the tunica intima/tunica media thickness ratio ($P < 0.05$). Nevertheless, LY reversed the effects of KGM on the thickness of aortic intima, foam cells, and lipids in the plaques, and the thickness of the tunica intima and the tunica intima/tunica media thickness ratio ($P < 0.05$). The results are shown in Fig. 5B–D.

3.6. Impacts of KGM and LY294002 on oxidative stress in rabbits with high-fat diet-induced atherosclerosis

To evaluate if KGM reduced the oxidative stress in rabbits with high-fat diet-induced atherosclerosis, the MPO activity and the levels of MDA, SOD and GSH-px were determined. KGM administration significantly decreased the concentrations of MPO and MDA, and increased the GSH-px and SOD concentrations compared to those in the HFD group. Interestingly, LY294002 administration inhibited the effect of KGM on mitigating oxidative stress (As illustrated in Fig. 6A–D.)

3.7. Impacts of KGM and LY294002 on PI3K/Akt in rabbits with high-fat diet-induced atherosclerosis

To further observe the underlying effects of the PI3K/Akt signal on the defensive roles of KGM, we determined the ratio of P-Akt/Akt and P-PI3K/PI3K. Compared with the CTR group, the ratios of P-Akt/Akt and P-PI3K/PI3K in the HFD group were significantly decreased ($P < 0.05$). Particularly, a noteworthy enhancement in P-AKT and P-PI3K protein expressions was observed in the KGM group ($P < 0.05$). Conversely, LY294002 administration blocked the activity of KGM on phosphorylation of PI3K and Akt ($P < 0.05$), indicating PI3K/Akt pathway is involved in the protective effect of KGM against high-fat diet-induced atherosclerosis. The results are shown in Fig. 7A–C.

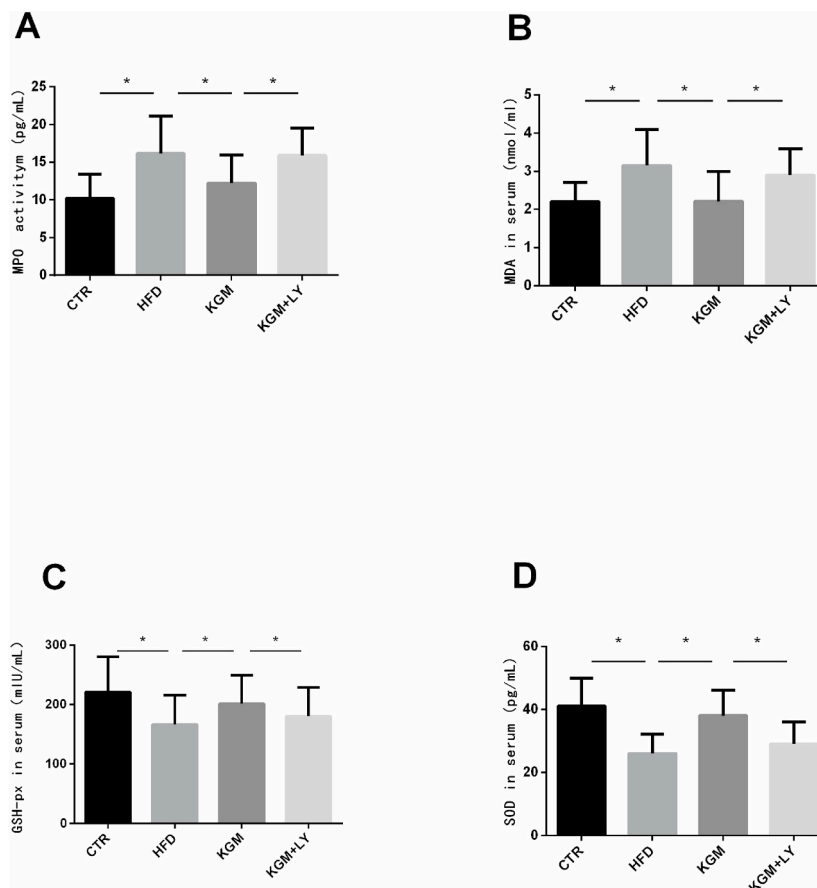


Fig. 6. Impacts of KGM and LY294002 on oxidative stress in rabbits with high-fat diet-induced atherosclerosis. The levels of MPO(A), MDA (B), SOD(C), and GSH-px(D) were analyzed by ELISA. The results are expressed as the mean \pm standard deviation ($n = 8$). * $P < 0.05$ vs. the indicated groups. KGM = konjac glucomannan.

4. Discussion

Atherosclerotic plaque is gradually formed by a series of pathophysiological processes leading to endothelial damage. Plasma lipids entering the arterial intima are deposited in the subintimal space; abnormal blood lipid levels, inflammatory response, and oxidative stress cause it [10]. In this study, we discovered that KGM displayed antiatherosclerosis effects, manifested by regulation blood lipids and suppression of inflammatory responses, endothelial injury, and oxidative stress. Notably, PI3K/Akt activity was confirmed to have a protective effect on KGM against high-fat diet-induced atherosclerosis. Our investigation elucidates the mechanism of KGM antagonizing against high-fat diet-induced atherosclerosis.

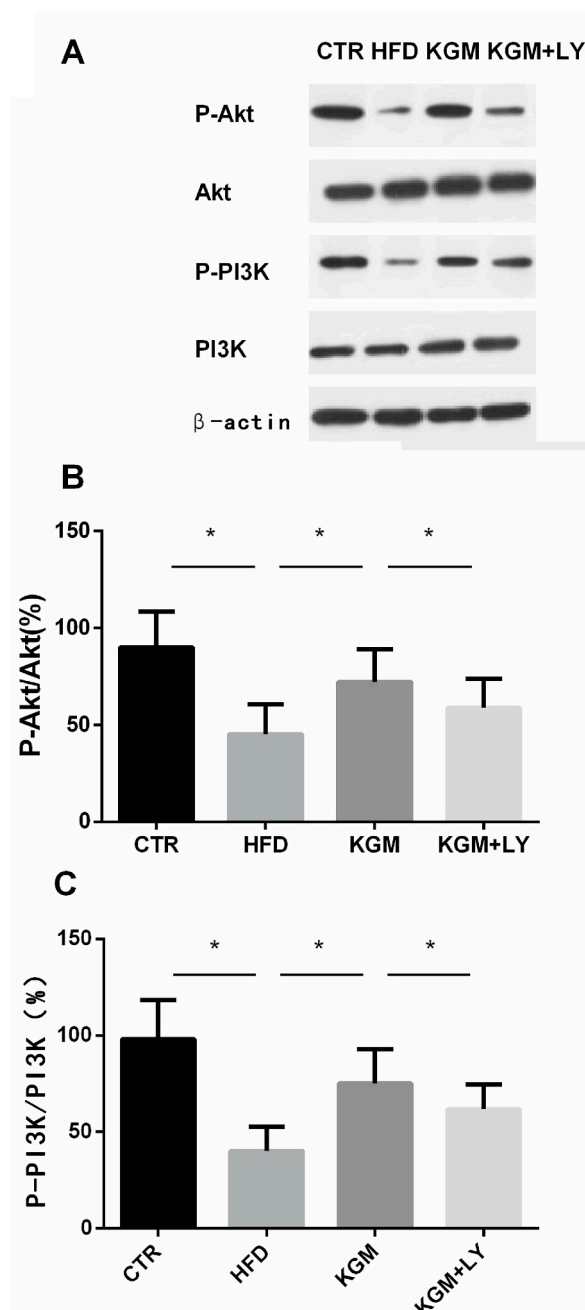


Fig. 7. Impacts of KGM and LY294002 on PI3K/Akt in rabbits with high-fat diet-induced atherosclerosis. (A) Akt, P-Akt, PI3K, and P-PI3K expression in the aortic wall was analyzed by Western blot. β -actin was used as the internal control. (B) Calculated P-Akt/Akt ratios. (C) Calculated P-PI3K/PI3K ratios. The results are expressed as the mean \pm standard deviation ($n = 8$). * $P < 0.05$ vs. the indicated groups. KGM = konjac glucomannan.

KGM has been shown to have an antiatherosclerosis effect [7]. This experiment used a high-fat diet fed to establish a rabbit model of atherosclerosis. After KGM administration, the degree of atherosclerosis was reduced, the plaques and foam cells were reduced, the lumen of the aorta was enlarged, and the tunica intima thickness and the tunica intima/tunica media thickness ratio in the aorta were significantly decreased. These results indicate that KGM alleviated atherosclerosis.

Elevated TC is an important independent risk factor for the occurrence of AS. Large-scale experiments have proven that a 10% reduction in total cholesterol can reduce the risk of coronary heart disease by 20%, and high LDL-C is a more important risk factor for AS [11]. HDL-C has a direct protective effect on the arterial walls and can promote the regression of atherosclerotic plaques [12]. Recent studies have shown that high TG may be no less of a risk factor than high LDL [13]. In addition, a series of large-scale clinical trials in recent years have also confirmed that drug-induced lipid regulation is an effective measure for primary and secondary prevention measure against coronary atherosclerotic cardiopathy [14]. This experiment confirmed that the administration of KGM decreased TC, TG, and LDL-C, and increased HDL-C. These results indicate that KGM functions in lipid regulation.

Atherosclerosis begins with vascular endothelial dysfunction and then progresses to lipid striations and plaque formation, and finally plaque rupture due to instability, during which process endothelial dysfunction is an important initial link that occurs throughout the whole process of atherosclerosis [15]. Therefore, improving vascular endothelial function has become the key to preventing atherosclerosis. Studies have shown that endothelial cells play a role in regulating vascular function by releasing vasodilator and constrictor factors and play an important role in thrombosis and the development of atherosclerotic plaques. NO is synthesized from L-arginine under the action of NOS in vascular endothelial cells, has a strong blood vessel-expanding function, maintains the body's blood coagulation fibrinolytic balance, reduces vascular endothelial permeability, reduces the expression of adhesion factors, inhibits platelet aggregation and smooth muscle proliferation and becomes a "protective factors" of endothelial cells [16,17]. ET is a vasoconstriction factor synthesized and secreted by vascular endothelial cells, that has a strong vasoconstriction effect and can also promote the proliferation and migration of smooth muscle cells, the mitotic response of fibroblasts, and promote the formation of atherosclerosis and restenosis [18]. ET and NO jointly maintain vascular tension, and their balance in the blood is of great significance in the prevention and treatment of atherosclerosis formation. The results of this experiment showed that the increase in ET and the decrease in NO in the HFD group broke the equilibrium state, and endothelial function injury promoted the occurrence and development of atherosclerosis. The significant decrease in ET and the significant increase in NO in the KGM group indicated that KGM could reduce atherosclerosis by improving vascular endothelial function.

Increasing evidence shows that atherosclerosis is an inflammation-proliferative disease, and the formation and progression of plaques are closely related to the inflammatory response [19,20]. CRP, TNF- α , and IL-6 are the hallmarks of inflammation, and lowering the level of CRP, TNF- α , and IL-6 can reduce coronary atherosclerosis. The results of this experiment showed that CRP, TNF- α , and IL-6 in the HFD group were significantly increased, while they in the KGM group were significantly decreased.

VCAM-1 is distributed on endothelial cells, which function is to mediate the adhesion of monocytes, lymphocytes, and neutrophils to endothelial cells. Increased expression of VCAM-1 was found in the lipid striae of early AS lesions in rabbits with hereditary hyperlipidemia and the arterial endothelial cells of cholesterol-fed mice. VCAM-1 is a potential marker of atherosclerosis [21]. The release of VCAM-1 from endothelial cells in early atherosclerosis promotes the migration of monocytes to the arterial wall, which plays a crucial role in the occurrence and development of atherosclerosis. The results of this experiment showed that KGM decreases the expression of VCAM-1. Therefore, it is speculated that KGM inhibits the progression of AS by inhibiting the expression of VCAM-1.

Oxidative stress-induced oxidative damage to endothelial cells is an important cause of endothelial dysfunction, which plays an important role in the development of AS [22]. Oxidative stress is involved in the occurrence of atherosclerosis, and inhibition of oxidative stress can alleviate AS [23]. Antioxidant therapy is considered a rational strategy to prevent atherosclerotic disease. One of the most effective ways to inhibit oxidative stress is the free removal of superoxide anions and hydrogen peroxide by increasing the expression of antioxidant proteins and antioxidant enzymes [24]. Our results demonstrated that KGM reduces AS by alleviating oxidative stress.

The upregulation of PI3K/AKT signaling pathway exerts a protective effect against AS in rats [25]. Zhou et al. [26] demonstrated that DHI treatment attenuates atherosclerosis and macrophage lipid accumulation by the activation of PI3K/AKT signaling pathway. When cells are stimulated, PI3K is phosphorylated to produce phosphatidylinositol-3 [3–5]-triphosphate (PIP3), which is the second messenger in Akt transport to the plasma membrane [27]. On the cell membrane, PIP3 promotes the phosphorylation of protein kinase B (Akt) to form P-Akt, which causes the proliferation of biological cells. P-Akt can be used as an indicator of PI3K activity [28]. Our experiment demonstrated that KGM administration enhances the expression of P-PI3K and P-Akt in high-fat diet-induced atherosclerosis, indicating that KGM activates the PI3K/Akt pathway.

To assess the role of the PI3K/AKT signaling pathway in the process by which KGM ameliorates atherosclerosis, we used LY294002, which is an inhibitor of PI3K/AKT [29], to administer high-fat diet-induced atherosclerosis. Our results demonstrated that the administration of LY294002 blocks the effects of KGM on inflammation, oxidative stress, endothelial function, blood lipids, and atherosclerosis, which indicates the PI3K/AKT signaling pathway involved in the process of KGM inhibits AS.

Despite these findings, there are some limitations to our study. First, this experiment was to investigate the effect of KGM preconditioning on atherosclerosis, rather than post-treatment. We will verify the protective effect of KGM postprocessing in subsequent experiments. Second, this trial is a study with a relatively small number of cases. A large trial is still needed to validate the efficacy of KGM in defense against high-fat diet-induced atherosclerosis.

5. Conclusion

The results demonstrated that KGM defends against high-fat diet-induced atherosclerosis by promoting PI3K/AKT pathway to

regulate blood lipids, and ameliorate inflammation, endothelial injury, VCAM-1, and oxidative stress in rabbits which provides a preliminary basis for large-scale clinical studies of KGM in the administration of AS patients in the future.

Ethics approval and consent to participate

Animal protocols were approved by the Ethics Committee of the Affiliated Hospital of Putian University.

Author contribution statement

Rongjie Guo; Junting Weng: Conceived and designed the experiments; Performed the experiments; Analyzed and interpreted the data; Contributed reagents, materials, analysis tools or data; Wrote the paper.

Min Chen: Conceived and designed the experiments; Analyzed and interpreted the data; Wrote the paper.

Bingbing Shi: Conceived and designed the experiments; Performed the experiments; Analyzed and interpreted the data; Wrote the paper.

Danjuan Liu: Conceived and designed the experiments; Performed the experiments; Contributed reagents, materials, analysis tools or data; Wrote the paper.

Shuoyun Weng: Conceived and designed the experiments; Analyzed and interpreted the data; Contributed reagents, materials, analysis tools or data; Wrote the paper.

Funding statement

PHD Junting Weng was supported by Natural Science Foundation of Fujian Province [2020J011253]; The Science and Technology Project of Putian City, Fujian Province [2020S3F008].

Data availability statement

The data that support the findings of this study are available in the supplementary material of this article.

Declaration of interest's statement

The authors declare no conflict of interest.

Appendix A. Supplementary data

Supplementary data to this article can be found online at <https://doi.org/10.1016/j.heliyon.2023.e13682>.

References

- [1] K. Kobiyama, K. Ley, Atherosclerosis. *Circulation research*. 123 (10) (2018) 1118–1120.
- [2] P. Libby, J.E. Buring, L. Badimon, G.K. Hansson, J. Deanfield, M.S. Bittencourt, et al., Atherosclerosis. *Nature reviews Disease primers*. 5 (1) (2019) 56.
- [3] E.A. Bohula, R.P. Giugliano, C.P. Cannon, J. Zhou, S.A. Murphy, J.A. White, et al., Achievement of dual low-density lipoprotein cholesterol and high-sensitivity C-reactive protein targets more frequent with the addition of ezetimibe to simvastatin and associated with better outcomes in IMPROVE-IT, *Circulation* 132 (13) (2015) 1224–1233.
- [4] D. Yang, Y. Yuan, L. Wang, X. Wang, R. Mu, J. Pang, et al., A review on konjac glucomannan gels: microstructure and application, *Int. J. Mol. Sci.* 18 (11) (2017).
- [5] R.D. Devaraj, C.K. Reddy, B. Xu, Health-promoting effects of konjac glucomannan and its practical applications: a critical review, *Int. J. Biol. Macromol.* 126 (2019) 273–281.
- [6] L. Yuan, J. Yu, J. Mu, T. Shi, Q. Sun, W. Jin, et al., Effects of deacetylation of konjac glucomannan on the physico-chemical properties of surimi gels from silver carp (*Hypophthalmichthys molitrix*), *RSC Adv.* 9 (34) (2019) 19828–19836.
- [7] H.V.T. Ho, E. Jovanovski, A. Zurbau, S. Blanco Mejia, J.L. Sievenpiper, F. Au-Yeung, et al., A systematic review and meta-analysis of randomized controlled trials of the effect of konjac glucomannan, a viscous soluble fiber, on LDL cholesterol and the new lipid targets non-HDL cholesterol and apolipoprotein B, *Am. J. Clin. Nutr.* 105 (5) (2017) 1239–1247.
- [8] H. Yan, Y. Ma, Y. Li, X. Zheng, P. Lv, Y. Zhang, et al., Insulin inhibits inflammation and promotes atherosclerotic plaque stability via PI3K-Akt pathway activation, *Immunol. Lett.* 170 (2016) 7–14.
- [9] Z. Liu, J. Li, S. Lin, Y. Wu, D. He, P. Qu, PI3K regulates the activation of NLRP3 inflammasome in atherosclerosis through part-dependent AKT signaling pathway, *Exp. Anim.* 70 (4) (2021) 488–497.
- [10] G.K. Hansson, Inflammation, atherosclerosis, and coronary artery disease, *N. Engl. J. Med.* 352 (16) (2005) 1685–1695.
- [11] C. Baigent, A. Keech, P.M. Kearney, L. Blackwell, G. Buck, C. Pollicino, et al., Efficacy and safety of cholesterol-lowering treatment: prospective meta-analysis of data from 90,056 participants in 14 randomised trials of statins, *Lancet (London, England)* 366 (9493) (2005) 1267–1278.
- [12] D. Duffy, D.J. Rader, Emerging therapies targeting high-density lipoprotein metabolism and reverse cholesterol transport, *Circulation* 113 (8) (2006) 1140–1150.
- [13] J. Ren, S.M. Grundy, J. Liu, W. Wang, M. Wang, J. Sun, et al., Long-term coronary heart disease risk associated with very-low-density lipoprotein cholesterol in Chinese: the results of a 15-Year Chinese Multi-Provincial Cohort Study (CMCS), *Atherosclerosis* 211 (1) (2010) 327–332.
- [14] Y. Wang, J. Liu, W. Wang, M. Wang, Y. Qi, W. Xie, et al., Lifetime risk for cardiovascular disease in a Chinese population: the Chinese Multi-Provincial Cohort Study, *Eur. J. Preven. Card.* 22 (3) (2015) 380–388.

- [15] J. Rathouska, K. Jezkova, I. Nemeckova, P. Nachtigal, Soluble endoglin, hypercholesterolemia and endothelial dysfunction, *Atherosclerosis* 243 (2) (2015) 383–388.
- [16] F.F. Hong, X.Y. Liang, W. Liu, S. Lv, S.J. He, H.B. Kuang, et al., Roles of eNOS in atherosclerosis treatment, *Inflamm. Res. : Off. J. Eur. Hist. Res. Soci.[et al]* 68 (6) (2019) 429–441.
- [17] Endothelial dysfunction in adults with obstructive sleep apnea, *Adv. Cardiol.* 46 (2011) 139–170.
- [18] N. Dhaun, D.J. Webb, Endothelins in cardiovascular biology and therapeutics, *Nat. Rev. Cardiol.* 16 (8) (2019) 491–502.
- [19] R.A. Brown, E. Shantsila, C. Varma, G.Y. Lip, Current understanding of atherogenesis, *Am. J. Med.* 130 (3) (2017) 268–282.
- [20] P.M. Ridker, B.M. Everett, T. Thuren, J.G. MacFadyen, W.H. Chang, C. Ballantyne, et al., Antiinflammatory therapy with canakinumab for atherosclerotic disease, *N. Engl. J. Med.* 377 (12) (2017) 1119–1131.
- [21] J.C.D. Santos, M.S. Cruz, R.H. Bortolin, K.M. Oliveira, J.N.G. Araújo, V.H.R. Duarte, et al., Relationship between circulating VCAM-1, ICAM-1, E-selectin and MMP9 and the extent of coronary lesions, *Clinics* 73 (2018), e203.
- [22] J. Huo, Z. Xu, K. Hosoe, H. Kubo, H. Miyahara, J. Dai, et al., Coenzyme Q10 prevents senescence and dysfunction caused by oxidative stress in vascular endothelial cells, *Oxid. Med. Cell. Longev.* 2018 (2018), 3181759.
- [23] M. Khosravi, A. Poursaleh, G. Ghasempour, S. Farhad, M. Najafi, The effects of oxidative stress on the development of atherosclerosis, *Biol. Chem.* 400 (6) (2019) 711–732.
- [24] X. Yang, Y. Li, Y. Li, X. Ren, X. Zhang, D. Hu, et al., Oxidative stress-mediated atherosclerosis: mechanisms and therapies, *Front. Physiol.* 8 (2017) 600.
- [25] X.L. Lu, C.H. Zhao, X.L. Yao, H. Zhang, Quercetin attenuates high fructose feeding-induced atherosclerosis by suppressing inflammation and apoptosis via ROS-regulated PI3K/AKT signaling pathway, *Biomed. Pharmacother.* 85 (2017) 658–671.
- [26] M. Zhou, P. Ren, S. Li, Q. Kang, Y. Zhang, W. Liu, et al., Danhong injection attenuates high-fat-induced atherosclerosis and macrophage lipid accumulation by regulating the PI3K/AKT insulin pathway, *J. Cardiovasc. Pharmacol.* 74 (2) (2019) 152–161.
- [27] M. Qin, Y. Luo, X.B. Meng, M. Wang, H.W. Wang, S.Y. Song, et al., Myricitrin attenuates endothelial cell apoptosis to prevent atherosclerosis: an insight into PI3K/Akt activation and STAT3 signaling pathways, *Vasc. Pharmacol.* 70 (2015) 23–34.
- [28] Z. Wang, Z. Bao, Y. Ding, S. Xu, R. Du, J. Yan, et al., Ne-carboxymethyl-lysine-induced PI3K/Akt signaling inhibition promotes foam cell apoptosis and atherosclerosis progression, *Biomed. Pharmacother.* 115 (2019), 108880.
- [29] P. Zhou, W. Xie, Y. Luo, S. Lu, Z. Dai, R. Wang, et al., Protective effects of total saponins of *Alaria elata* (miq.) on endothelial cell injury induced by TNF- α via modulation of the PI3K/Akt and NF- κ B signalling pathways, *Int. J. Mol. Sci.* 20 (1) (2018).